OPEN

Citation: Bone Research (2014) 2, 14038; doi:10.1038/boneres.2014.38
© 2014 Sichuan University. All rights reserved 2095-4700/14
www.nature.com/boneres

ARTICLE

Deletion of IFT20 in early stage T lymphocyte differentiation inhibits the development of collagen-induced arthritis

Xue Yuan[1], Lee Ann Garrett-Sinha[2], Debanjan Sarkar[3] and Shuying Yang[1,4]

IFT20 is the smallest member of the intraflagellar transport protein (IFT) complex B. It is involved in cilia formation. Studies of IFT20 have been confined to ciliated cells. Recently, IFT20 was found to be also expressed in non-ciliated T cells and have functions in immune synapse formation and signaling *in vitro*. However, how IFT20 regulates T-cell development and activation *in vivo* is still unknown. We deleted the *IFT20* gene in early and later stages of T-cell development by crossing *IFT20*$^{flox/flox}$ (*IFT20*$^{f/f}$) mice with Lck-Cre and CD4-Cre transgenic mice, and investigated the role of IFT20 in T-cell maturation and in the development of T cell-mediated collagen-induced arthritis (CIA). We found that both *Lck-Cre/IFT20*$^{f/f}$ and *CD4-Cre/IFT20*$^{f/f}$ mice were indistinguishable from their wild-type littermates in body size, as well as in the morphology and weight of the spleen and thymus. However, the number of CD4- and CD8-positive cells was significantly lower in thymus and spleen in *Lck-Cre/IFT20*$^{f/f}$ mice. Meanwhile, the incidence and severity of CIA symptoms were significantly decreased, and inflammation in the paw was significantly inhibited in *Lck-Cre/IFT20*$^{f/f}$ mice compared to *Lck-Cre/IFT20*$^{+/+}$ littermates. Deletion *IFT20* in more mature T cells of *CD4-Cre/IFT20*$^{f/f}$ mice had only mild effects on the development of T cells and CIA. The expression of IL-1β, IL-6 and TGF-β1 were significantly downregulated in the paw of *Lck-Cre/IFT20*$^{f/f}$ mice, but just slight decreased in *CD4-Cre/IFT20*$^{f/f}$ mice. These results demonstrate that deletion of *IFT20* in the early stage of T-cell development inhibited CIA development through regulating T-cell development and the expression of critical cytokines.

Bone Research (2014) **2,** 14038; doi:10.1038/boneres.2014.38; Published online: 18 November 2014

INTRODUCTION

Intraflagellar transport (IFT) proteins are a group of proteins which were first found to be essential for cilia formation.[1–2] So far, 20 IFT proteins have been identified. These proteins form intraflagellar transport complex A (IFT-A) and complex B (IFT-B).[3] IFT-A contains six proteins (IFT144, IFT140, IFT139, IFT122, IFT121 and IFT43)[4–6] and IFT-B contains fourteen proteins (IFT20, IFT22, IFT25, IFT27, IFT46, IFT52, IFT54, IFT57, IFT70, IFT74/IFT72, IFT80, IFT81, IFT88 and IFT172).[4,6–8] IFT proteins cooperate with IFT motors (kinesin and dynein) to drive macromolecules from the base to the tip of the cilium (anterograde transport) and from the tip of the cilium back to the cell body (retrograde transport).[9]

IFT20 is the smallest of the IFT complex B proteins, and has several unique features. IFT20 is anchored to the Golgi complex by Golgin protein, i.e., Golgi Microtubule Associated Protein 210/thyroid hormone receptor interacting protein 11. IFT20 is involved in ciliary protein sorting,[10–11] and also exhibits strong interactions with IFT57/Hippi and kinesin II subunit Kif3b, indicating its role in IFT complex and motor assembly.[12] Hematopoietic stem cells have been believed to lack of IFT protein related signaling due to lack cilia.[13] Recently, however, a breakthrough discovery was made by Finetti *et al.*[14] showing that IFT20 is expressed in lymphoid and myeloid cells, indicating that IFT20 has functions independent of cilia formation. They demonstrated that IFT20 is involved in the polarized recycling of the T-cell receptor (TCR)/CD3 complex, which connects IFT with membrane trafficking.[14] When antigen-presenting cells present antigens to T cells, IFT20 promotes polarized recycling and clustering of the TCR at the immune synapse. Knockdown of IFT20 in T cells blocks both

[1]Department of Oral Biology, School of Dental Medicine, University at Buffalo, The State University of New York, Buffalo, NY 14214, USA; [2]Department of Biochemistry, School of Medicine and Biomedical Sciences, University at Buffalo, The State University of New York, Buffalo, NY 14203, USA; [3]Laboratory for Biomaterials and Regenerative Therapeutics, Department of Biomedical Engineering, University at Buffalo, The State University of New York, Buffalo, NY 14260-2050, USA and [4]Developmental Genomics Group, New York State Center of Excellence in Bioinformatics and Life Sciences, University at Buffalo, The State University of New York, Buffalo, NY 14203, USA
Correspondence: SY Yang (sy47@buffalo.edu)
Received: 6 May 2014; Revised: 26 September 2014; Accepted: 28 September 2014

constitutive TCR recycling and the polarization of TCR recycling to the immune synapse.[14] These novel findings demonstrated that IFT20 is a regulator of immune synapse assembly in T cells *in vitro*. However, how IFT20 regulates T cell development and function *in vivo* is largely unknown.

A mouse *IFT20* floxed allele (*IFT20*$^{f/f}$) has been described by Jonassen *et al*.[15] Germline deletion of *IFT20* with Prm-Cre causes embryonic lethality.[15] So far, only HoxB7-Cre and human red/green pigment gene promoter-Cre have been used to study the role of IFT20 in kidney and photoreceptor cells.[15–16] In order to study the role of IFT20 in T cells *in vivo*, we deleted *IFT20* in early and later stages of T-cell development by crossing *IFT20*$^{f/f}$ mice with Lck-Cre or CD4-Cre transgenic mice, respectively, to generate T cell-specific *IFT20* knockout mouse models.

Rheumatoid arthritis (RA) is a systemic autoimmune disease accompanied by synovial inflammation and destruction of joints.[17] In order to uncover the pathogenesis of RA, several arthritis mouse models have been established, including collagen-induced arthritis (CIA), antigen-induced arthritis, collagen antibody-induced arthritis and TNF-α transgenic mouse model of inflammatory arthritis.[18–20] CIA is the most widely used experimental model of RA and recently has been extensively studied to identify the pathogenic mechanism of RA and to examine the effects of therapeutics. Type II collagen is exclusively expressed in the articular cartilage. Autoimmune response to type II collagen offers a validated mechanism by which the immune system contributes to the pathogenesis of RA in human patients. Therefore, the mouse CIA model shares both immunological and pathological features with human RA. Although both T cell- and B cell-specific responses to type II collagen contribute to immunopathogenesis of CIA, T cells are known to play critical roles in CIA initiation and disease perpetuation.[21] Defects in T cells have been shown to block the CIA initiation and development in mouse models.[22–24]

Considering the potential role of IFT20 in TCR/CD3 recycling during T-cell activation, it is interesting to investigate whether deletion of IFT20 in the T-cell lineage affects CIA initiation and development. In this study, we challenged *Lck-Cre/IFT20*$^{f/f}$ and *CD4-Cre/IFT20*$^{f/f}$ mice with type II chicken collagen and analyzed CIA pathogenesis. We explored the role of IFT20 in T cells *in vivo* by comparing the incidence and the intensity of CIA in *Lck-Cre/IFT20*$^{f/f}$ and *CD4-Cre/IFT20*$^{f/f}$ mice with their wild-type littermates. Our results demonstrate that specific deletion of IFT20 in T cells with Lck-Cre or CD4-Cre did not lead to any gross changes in phenotypes such as body weight or the morphology and weight of spleen and thymus. However, specific deletion of *IFT20* at an early stage of T-cell differentiation with Lck-Cre significantly reduced CD4- and CD8-positive cells in both the thymus and spleen. Additionally, these mice showed significantly reduced incidence and severity of CIA. Unexpectedly, deletion of *IFT20* with CD4-Cre showed minor effect on CD4- and CD8-positive cell population and CIA development. This data suggests the complicated role of IFT20 in T-cell development and activation.

MATERIALS AND METHODS

Mice

IFT20$^{f/f}$ mice, Lck-Cre mice, and CD4-Cre mice were all purchased from the Jackson Laboratory (Bar Harbor, ME, USA). *IFT20*$^{f/f}$ mice have been previously described.[25] Mice carrying the *IFT20*^{flox} allele were crossed with Lck-Cre mice or CD4-Cre mice in order to delete exons 2 and 3 and create *Lck-Cre/IFT20*$^{f/f}$ and *CD4-Cre/IFT20*$^{f/f}$ mice. Homozygous *Lck-Cre/IFT20*$^{f/f}$ and *CD4-Cre/IFT20*$^{f/f}$ mice are viable. Mouse genotyping was done by polymerase chain reaction (PCR) of proteinase K-digested toe DNA as we have previously described[26] by using two primers IFT20F (5′-ACT CAG TAT GCA GCC CAG GT-3′) and IFT20R (5′-GCT AGA TGC TGG CGT AAA G-3′), which yielded a 506 bp band for the flox allele and a 404 bp band for wild-type allele.[25] The presence of the Lck-Cre and CD4-Cre transgene was detected with the following primers CREF (5′-CCT GGA AAA TGC TTC TGT CCG TTT GCC-3′) and CREB (5′-GGC GCG GCA ACA CCA TTT TT-3′), which generated a PCR product of 550 bp. Mouse studies were approved by University at Buffalo Institutional Animal Care and Use Committee.

Isolation of T cells from spleen

T cells were isolated from total spleen cells of *Lck-Cre/IFT20*$^{+/+}$, *Lck-Cre/IFT20*$^{f/f}$, *CD4-Cre/IFT20*$^{f/f}$ and *CD4-Cre/IFT20*$^{f/f}$ mice using a pan T-cell isolation kit (mouse; Miltenyi Biotec Inc., Auburn, CA, USA) following the manufacturer's instruction. T cells and non-T cells were used for *IFT20* expression analysis by quantitative real-time polymerase chain reaction (qPCR).

Flow cytometry

Spleen and thymus were harvested from *Lck-Cre/IFT20*$^{+/+}$, *Lck-Cre/IFT20*$^{f/f}$, *CD4-Cre/IFT20*$^{f/f}$ and *CD4-Cre/IFT20*$^{f/f}$ mice. Single cell suspensions were prepared by crushing the spleen or thymus, followed by passing through an 18.5 gauge needle three times. The cells were resuspended in 0.2% BSA–PBS and exposed to Fc block (anti-CD16/32; BD Pharmingen) for 15 min. Then, PE tagged anti-CD4 (553652; BD Pharmingen) and antigen-presenting cell-tagged anti-CD8 (553035; BD Pharmingen) were added. After 20 min incubation in the dark, the cells were washed and processed using a BD LSRFortessa flow cytometry machine.

Collagen-induced arthritis

CIA was induced following the protocol from Chondrex (Redmond, WA, USA). In brief, mice were immunized with

© 2014 Sichuan University

100 μL of 2 mg·mL^{-1} chicken type II collagen (Cat. No. 20012; Chondrex) emulsified in Complete Freund's Adjuvant (CFA, Cat. No. 7023; Chondrex) containing 5 mg·mL^{-1} *M. tuberculosis* intradermally at the base of the tail on day 0. On day 21, the mice were given booster injection with the same amount of chicken type II collagen and CFA intradermally at the base of the tail.[18]

Evaluation of arthritis severity

To quantitatively evaluate the severity of the arthritis, an arthritis score was evaluated every 3 days for as long as 66 days after the first immunization. Inflammation of the four paws was assessed by using the following scale from 0 to 4: grade 0, normal; grade 1, slight redness and swelling of the ankle or wrist; grade 2, moderate redness and swelling of ankle or wrist; grade 3, extensive redness and swelling of the entire paw including digits; grade 4, maximally inflamed limb with involvement of multiple joints showing joint distortion and/or rigidity. The maximum score per mouse was 16. Mouse with clinical score greater than 4 was given a diagnosis of arthritis. The mean arthritic score was determined in arthritic animals only.[27–29]

Paw thickness measurement

The thickness of hind paws was measured using Precision Vernier Calipers (General, New York, NY, USA) and recorded 60 days after first immunization.[30]

Histological assessment of arthritis

For histological analysis, mice were sacrificed at day 66 after the first immunization. Hind paws were collected and fixed in 10% neutral formalin, decalcified with 10% EDTA for 1 week and embedded in paraffin. Then, 5-μm slices were prepared and stained with hematoxylin and eosin.[2] The joint sections were graded for disease severity using a scoring system from 0 to 4:[31–32] grade 0, normal ankle joint; grade 1, normal synovium with few mononuclear cells; grade 2, a few layers of flat to rounded synovial lining cells and dense infiltration with mononuclear cells; grade 3, hyperplasia of the synovium with mononuclear cells infiltration; and grade 4, severe synovitis with pannus and articular cartilage destruction.

Thymus and spleen assays

Thymus and spleen were removed and weighed immediately after mice were killed at the end of the experiments. The thymus index was calculated as the ratio of thymus weight to mouse body weight (mg·g^{-1}) and the spleen index was calculated as the ratio of spleen weight to mouse body weight (mg·g^{-1}).[28,33]

qPCR

Paws were quickly frozen in liquid nitrogen and ground with Trizol reagent using a chilled mortar and pestle for quality RNA isolation (Invitrogen, Carlsbad, CA, USA), following the manufacturer's instructions. cDNA was synthesized from 2 μg total RNA using RNA to cDNA EcoDry Premix kit (Clontech, Palo Alto, CA, USA). qPCR was performed with ABI PRISM 7500 real time PCR system (Invitrogen) using SYBR Green PCR master Mix (Invitrogen). Sequences and product lengths for each primer pair were as follows: IFT20 (forward: 5′-AGA AGC AGA GAA CGA GAA GAT G-3′; reverse: 5′-CAC AAA GCT TCA TAT TCA ACC CG-3′, 156 bp); IL-1β (forward: 5′-ACA GAT GAA GTG CTC CTT CCA-3′; reverse: 5′-GTC GGA GAT TCG TAG CTG GAT-3′, 73 bp);[34] IL-6 (forward: 5′-ATG GAT GCT ACC AAA CTG GAT-3′; reverse: 5′-TGA AGG ACT CTG GCT TTG TCT-3′, 139 bp)[35] and TGF-β (forward: 5′-TGA CGT CAC TGG AGT TGT ACG G-3′; reverse: 5′-GGT TCA TGT CAG GAT GGT GC-3′, 170 bp).[36] All of the reactions were run in triplicate and normalized to the housekeeping gene GAPDH.

Statistical analysis

All data were represented as mean±standard deviation (s.d.). Differences between groups were evaluated by unpaired, two-tailed Student's *t*-test. *P* values less than 0.05 were considered to be significant.

RESULTS

Deletion of *IFT20* in different stages of T-cell development showed normal Mendelian genetics and normal phenotypes

To investigate the roles of IFT20 in T cells, we generated T cell-specific *IFT20* knockout mice, as described in the section on 'Materials and methods'. Mice harboring loxP sites flanking the second and third exons of *IFT20* gene (*IFT20*$^{f/f}$) were crossed with Lck-Cre or CD4-Cre transgenic mice (Figure 1a). Cre recombinase-mediated deletion removed the start codon and 71 of 132 codons of *IFT20* gene and produced a null mutant allele.[25] Genotyping of mice was performed by PCR analysis (Figure 1b). The bands of 506 bp represent the *IFT20*^{flox} allele while the bands of 404 bp represent the wild-type allele (*IFT20*$^{+}$). The 550 bp bands indicate that the Cre gene is present allowing Cre-mediated deletion the target gene. Both Lck-Cre and CD4-Cre transgenic lines are T cell-specific targeted Cre, which are known to delete target genes at early and later stages of thymocyte differentiation (Figure 1a). Double-negative (DN, CD4^{-}CD8^{-}) thymocytes go through four developmental stages (DN1 to DN4), which are distinguishable by their surface markers.[37] Lck promoter activity is first detected at the DN2 stage,[38] and the Lck-Cre transgene is expressed during early intrathymic development in the thymus.[38–39] CD4 is first expressed in the CD4^{+}CD8^{+} double-positive (DP) thymocyte stage and, therefore, the CD4-Cre transgene is not expressed until a later stage of thymic

© 2014 Sichuan University

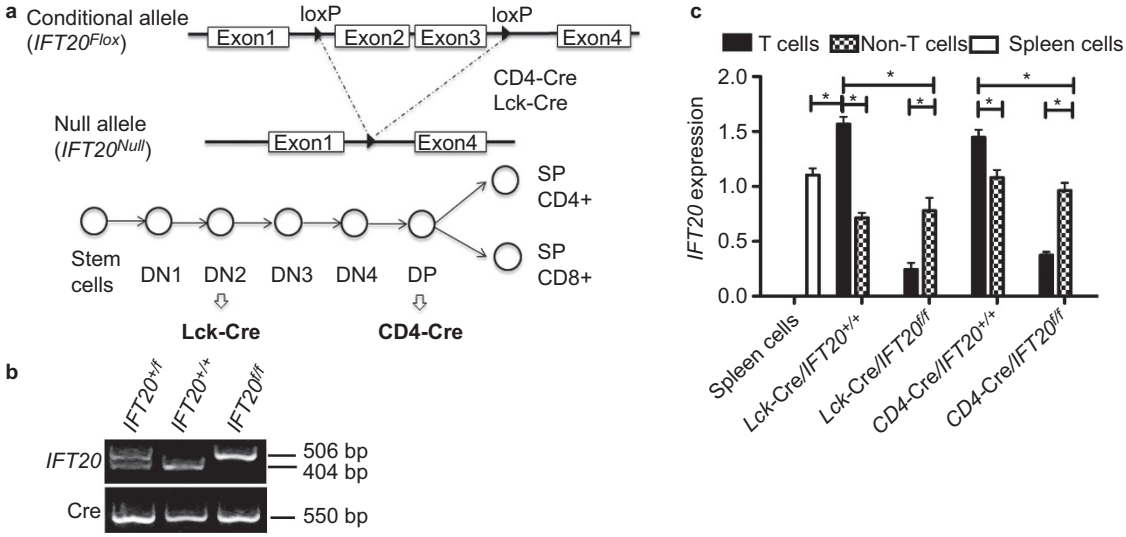

Figure 1. Deletion of IFT20 in different stages of T-cell development showed normal Mendelian genetics and normal phenotypes. (**a**) Structure of *IFT20*^{flox} and *IFT20*^{Null} alleles. Two loxP sites were inserted into IFT20 locus flanking exon2 and exon3. Lck-Cre or CD4-Cre mediated the excision of exons 2 and 3 and converted *IFT20*^{flox} to *IFT20*^{Null}. Lck-Cre and CD4-Cre are T cell-specific Cre transgenes driven either by Lck or CD4 promoter. The stages of thymocyte differentiation where the proximal Lck and CD4 promoters are active are indicated. DN: double negative; DP: double positive. (**b**) Genotyping showed wild-type and conditional alleles as well as the Cre recombinase transgene. The sequence of primers is given in the section on 'Materials and methods'. (**c**) qPCR analysis shows less IFT20 mRNA expression in T cells from *Lck-Cre/IFT20*$^{f/f}$ and *CD4-Cre/IFT20*$^{f/f}$ spleen. The expression of IFT20 was normalized to GAPDH expression (*$P<0.001$ *versus* controls). Spleen cells: spleen cells from wild-type mouse; T cells: sorted T cells from spleen; non-T cells: other cells in spleen.

development.[38] To detect the *IFT20* deletion in T cells, total T cells were harvested from the spleen of *Lck-Cre/IFT20*$^{+/+}$, *Lck-Cre/IFT20*$^{f/f}$, *CD4-Cre/IFT20*$^{f/f}$ and *CD4-Cre/IFT20*$^{+/+}$ mice using the pan T-cell isolation kit. T cells were negatively selected and lysed with Trizol. Non-T cells were also harvested and used as a control. In mice without Cre, expression of IFT20 was about 1.5- to 2-fold higher in the T-cell population than the non-T-cell population of

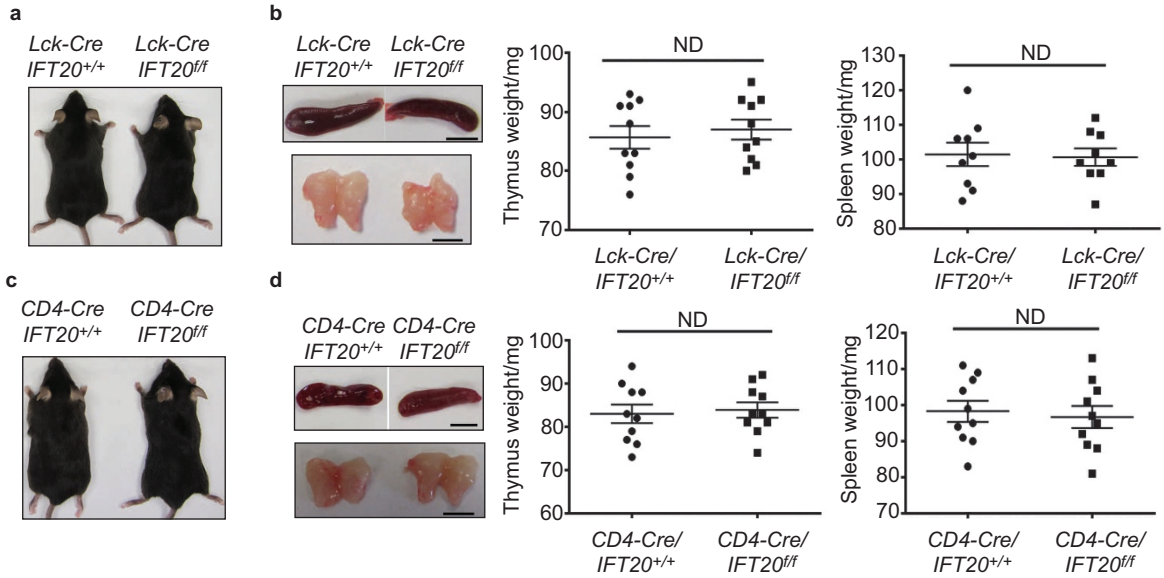

Figure 2. Both *Lck-Cre/IFT20*$^{f/f}$ and *CD4-Cre/IFT20*$^{f/f}$ mice were indistinguishable from wild-type littermates in mouse body size, and in the morphology and weights of the spleen and thymus. (**a**) Representative photograph of *Lck-Cre/IFT20*$^{+/+}$ and *Lck-Cre/IFT20*$^{f/f}$ mice at 3 months of age showing similar body mass and appearance. (**b**) Thymus and spleen from *Lck-Cre/IFT20*$^{f/f}$ mice shown next to those from a *Lck-Cre/IFT20*$^{+/+}$ littermate. Similar *Lck-Cre/IFT20*$^{f/f}$ thymic weight was found compared to age-matched *Lck-Cre/IFT20*$^{+/+}$ ($n=10$, $P>0.05$) (**c**) Representative photograph of *CD4-Cre/IFT20*$^{+/+}$ and *CD4-Cre/IFT20*$^{f/f}$ mice at 3 months of age showing similar body mass and appearance. (**d**) Thymus and spleen from *CD4-Cre/IFT20*$^{f/f}$ mice shown next to those from a *CD4-Cre/IFT20*$^{+/+}$ littermate. Similar *Lck-Cre/IFT20*$^{f/f}$ thymic weight was observed compared to *CD4-Cre/IFT20*$^{+/+}$ littermate ($n=10$, $P>0.05$) ND, no significant difference.

© 2014 Sichuan University

the spleen (Figure 1c). This suggests that T cells express more IFT20 than do non-T cells in the spleen (which comprise in large part B cells) and supports the idea that IFT20 may play a special role in T-cell development. IFT20 expression was significantly reduced (5- to 10-fold) in the T cells of *Lck-Cre/IFT20*$^{f/f}$ mice compared to that in the T cells from *Lck-Cre/IFT20*$^{f/f}$ mice (Figure 1c). IFT20 expression was also significantly reduced in the T cells of *CD4-Cre/IFT20*$^{f/f}$ mice compared to that in the T cells from *CD4-Cre/IFT20*$^{+/+}$ mice. However, IFT20 expression in T cells from *CD4-Cre/IFT20*$^{f/f}$ mouse was slightly (but not significantly) higher than that from *Lck-Cre/IFT20*$^{f/f}$.

Lck-Cre/IFT20$^{f/f}$ and *CD4-cre/IFT20*$^{f/f}$ mice were born at normal Mendelian ratios and appeared normal (Figure 2a and 2c). Further analysis of spleen and thymus weights did not reveal any abnormalities. The spleens and thymuses in *Lck-Cre/IFT20*$^{f/f}$ and *CD4-Cre/IFT20*$^{f/f}$ mice have similar weights compared to wild-type control littermates (Figure 2b and 2d).

Deletion of *IFT20* in an early stage of T-cell differentiation reduced the population of CD4- and CD8-positive cells

To investigate the role of *IFT20* in T-cell development, we detected the CD4- and CD8-positive cells in both thymus and spleen with flow cytometry. As shown in Figure 3a and 3b, depletion of *IFT20* in the beginning of DP stage with Lck-Cre resulted in a significant loss of $CD4^+$, $CD8^+$ and $CD4^+CD8^+$ T cells in the spleen, while it increased the $CD4^-CD8^-$ population. In the thymus, the $CD4^+$ and $CD8^+$ T cells were also significantly reduced, accompanied by increased $CD4^-CD8^-$ cell numbers. However, the numbers of CD4 and CD8 single- and double-positive T cells were not apparently affected when *IFT20* was deleted with CD4-Cre (Figure 3c and 3d), indicating that the loss of *IFT20* in DP stage does not significantly alter thymocyte differentiation. These findings suggest that IFT20 may function in DN proliferation, but is not required for further differentiation.

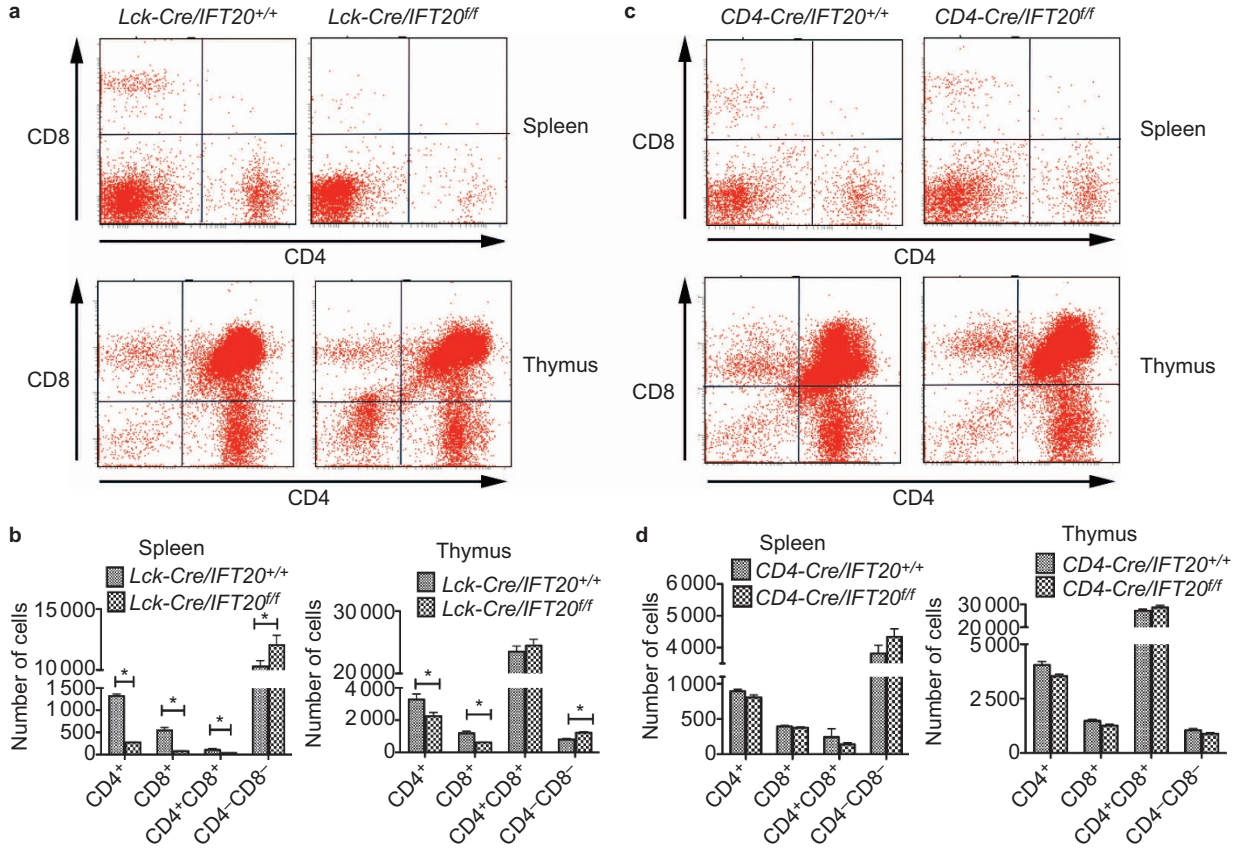

Figure 3. Deletion *IFT20* in double-negative thymocytes affected the T-cell development. (**a**) Thymuses and spleens were collected from 1-month-old *Lck-Cre/IFT20*$^{+/+}$ and *Lck-Cre/IFT20*$^{f/f}$ mice; the cells were analyzed by flow cytometry for CD4 and CD8 expression. In the flow cytometry pictures: top left represents $CD8^+CD4^-$ cells; top right represents $CD8^+CD4^+$ cells; bottom left represents $CD8^-CD4^-$ cells; and bottom right represents $CD8^-CD4^+$ cells. (**b**) Number of CD4 single-positive ($CD4^+$), CD8 single-positive ($CD8^+$), CD4 and CD8 double-positive ($CD4^+CD8^+$), and CD4 and CD8 double-negative ($CD4^-CD8^-$) (n=4, *P<0.01). (**c**) Flow cytometry of cells from thymuses and spleens of *CD4-Cre/IFT20*$^{+/+}$ and *CD4-Cre/IFT20*$^{f/f}$ mice. (**d**) Number of CD4 single-positive ($CD4^+$), CD8 single-positive ($CD8^+$), CD4 and CD8 double-positive ($CD4^+CD8^+$) and CD4 and CD8 double-negative ($CD4^-CD8^-$) (n=4).

© 2014 Sichuan University

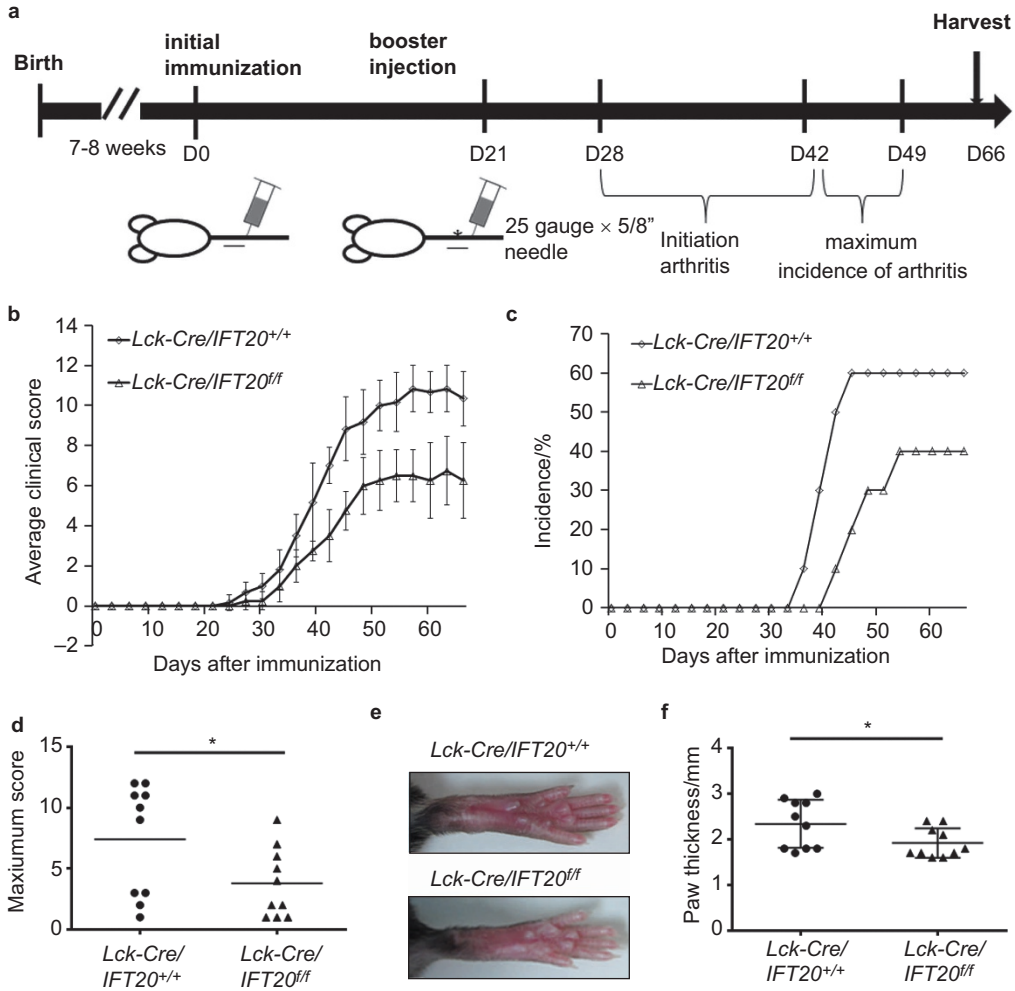

Figure 4. Deletion IFT20 in double-negative thymocytes affected the development of CIA. (**a**) Timeline for the CIA mouse model. Seven- to eight-week-old mice were immunized with 100 μL emulsion containing equal volume of CFA (including 5 mg·mL^{-1} of *M. tuberculosis*) and chicken type II collagen solution (2 mg·mL^{-1} in 0.05 mol·mL^{-1} acetic acid). The booster injection (Insert site: 3 cm from the base of the tail Injection site: 1.5 cm from the base) was made with the same emulsions 21 days after initial injection (Insert site: 2 cm from the base of the tail Injection site: 0.5 cm from the base). Arthritis usually can be observed 4–6 weeks after the first immunization with the maximum incidence of arthritis at 6–7 weeks. All the experimental mice were harvested at day 66 for the histological analysis. (**b**) Mean clinical scores±s.d. of arthritis in *Lck-Cre/IFT20*$^{+/+}$ (n=6) and *Lck-Cre/IFT20*$^{f/f}$ mice (n=4) with arthritis (P<0.01 after day 40). (**c**) Percentage of mice of *Lck-Cre/IFT20*$^{+/+}$ and *Lck-Cre/IFT20*$^{f/f}$ mice that developed arthritis (n=10, P<0.05 after day 40). (**d**) The maximum clinical score was recorded until day 66 (n=10, *P<0.01). (**e**) Hind paws of type II collagen immunized *Lck-Cre/IFT20*$^{+/+}$ and *Lck-Cre/IFT20*$^{f/f}$ mice. (**f**) The hind paw thickness was measured at day 66 to indicate arthritis development (n=10, *P<0.01).

Deletion of *IFT20* at an early stage of T-cell differentiation suppressed the development of CIA

To determine the functional role of IFT20 in T cell-mediated inflammatory diseases, we created the CIA model in wild-type and *IFT20* mutant mice. The C57/BL6 strain has been considered to be a CIA-resistant strain, due to little or no incidence of CIA upon immunization.[18,40] However, Campbell *et al*.[27] successfully induced arthritis at relatively high incidence in CIA-resistant mouse strains, such as C57BL/6, C57BL/10, and 129/Sv mice (H-2b) with CFA, which contains 5 mg·mL^{-1} of *M. tuberculosis*. We used this CIA model with a slight modification, and the immunization schedule followed is shown in Figure 4a. Six- to seven-week-old, age-matched *Lck-Cre/IFT20*$^{+/+}$ and *Lck-Cre/IFT20*$^{f/f}$ C57BL/6 mice were chosen for generating the CIA model. Stable emulsions with an equal volume of CFA (containing 5 mg·mL^{-1} of *M. tuberculosis*) and chicken type II collagen solution (2 mg·mL^{-1} in 0.05 mol·mL^{-1} acetic acid) were prepared immediately before the injection on day 0 (initial immunization) and day 21 (booster injection). Each mouse received an accurate 0.1 mL of the emulsion each time. For the initial immunization, the injection site was 2 cm from the base of the tail, and a 25 gauge×5/8″ needle was used to reach to 0.5 cm from the base for injection. The booster injection was inserted at 3 cm from the base of the tail until the needle tip reached 1.5 cm from the base (Figure 4a). The needle was wiped and inserted bevel up and parallel to the tail in order to prevent leakage of emulsion. We

© 2014 Sichuan University

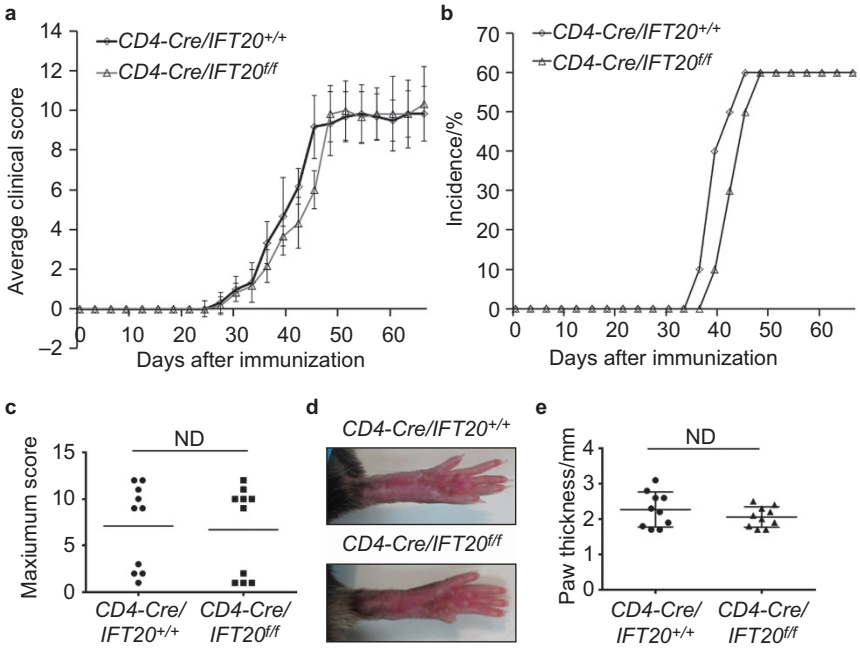

Figure 5. Deletion of *IFT20* in more mature T cells had only mild effects on the development of CIA. (**a**) Mean clinical scores±s.d. of arthritis in *CD4-Cre/IFT20*$^{+/+}$ (n=6) and *CD4-Cre/IFT20*$^{f/f}$ mice (n=6) immunized with chicken type II collagen emulsified in CFA. (**b**) Percentage of *CD4-Cre/IFT20*$^{+/+}$ mice and *CD4-Cre/IFT20*$^{f/f}$ mice that developed arthritis (n=10). (**c**) The maximum clinical score was recorded until day 66 (n=10). (**d**) Hind paws of type II collagen immunized *CD4-Cre/IFT20*$^{+/+}$ and *CD4-Cre/IFT20*$^{f/f}$ mice. (**e**) The hind paw thickness was measured at day 66 to indicate arthritis development (n=10). ND indicates no significant difference.

observed arthritis at week 5 after the first immunization. The maximum incidence of arthritis was achieved at 6–7 weeks. To quantitatively evaluate the severity of the arthritis, four paws were observed and measured every 3 days up to 66 days after the first immunization using the grades as described in the section on 'Materials and methods'. The incidence of CIA was significantly lower in the *Lck-Cre/IFT20*$^{f/f}$ group than that in the *Lck-Cre/IFT20*$^{+/+}$ group (Figure 4c). Even during development of the arthritis, the severity of the disease in *Lck-Cre/IFT20*$^{f/f}$ mice was much less than that in *Lck-Cre/IFT20*$^{+/+}$ mice (Figure 4b and 4c). The hind paw of *Lck-Cre/IFT20*$^{+/+}$ displayed severe joint inflammation evidenced by marked swelling and erythema of paws (Figure 4e). In contrast, *Lck-Cre/IFT20*$^{f/f}$ mice were resistant to developing CIA and showed no signs or only slight signs of paw and/or joint swelling (Figure 4e). The thickness of hind paws was measured at the end of the experiment. *Lck-Cre/IFT20*$^{f/f}$ mice had significantly thinner paws than *Lck-Cre/IFT20*$^{+/+}$ mice, which confirmed that the development and severity of CIA was reduced in *Lck-Cre/IFT20*$^{f/f}$ mice (Figure 4f).

Deletion *IFT20* in more mature T cells had only mild effects on the development of CIA

To further determine the role of IFT20 in T cells, *CD4-Cre/IFT20*$^{f/f}$ and *CD4-Cre/IFT20*$^{+/+}$ mice were subjected to CIA induction. Although *CD4-Cre/IFT20*$^{f/f}$ mice showed a delay in the development of arthritis, the incidence of CIA was similar in the *CD4-Cre/IFT20*$^{f/f}$ group compared to the *CD4-Cre/IFT20*$^{+/+}$ group (Figure 5b). Average clinical scores and maximum scores were not significantly different between *CD4-Cre/IFT20*$^{f/f}$ mice and *CD4-Cre/IFT20*$^{+/+}$ mice during the development of arthritis (Figure 5a and 5c). The hind paws of *CD4-Cre/IFT20*$^{+/+}$ mice and *CD4-Cre/IFT20*$^{f/f}$ mice displayed swelling and erythema with similar paw thicknesses (Figure 5d and 5e).

Deletion of *IFT20* protected against histopathological progression of arthritis in *Lck-Cre/IFT20*$^{f/f}$ mice, but not in *CD4-Cre/IFT20*$^{f/f}$

In the histological analysis, the affected joints of *Lck-Cre/IFT20*$^{+/+}$ mice and *CD4-Cre/IFT20*$^{+/+}$ mice showed typical features of arthritis, characterized by synovial hyperplasia and perivascular infiltration of inflammatory cells. In severely affected joints, there was marked cartilage destruction (Figure 6a and 6d). However, the joints of *Lck-Cre/IFT20*$^{f/f}$ mice did not have any significant sign of tissue degeneration or inflammation. In contrast, both *CD4-Cre/IFT20*$^{+/+}$ and *CD4-Cre/IFT20*$^{f/f}$ mice showed a similar level of joint inflammation and articular cartilage degeneration (Figure 6d). Semiquantitative scoring of these histological parameters confirmed that arthritic severity in *CD4-Cre/IFT20*$^{f/f}$ was comparable to that of *CD4-Cre/IFT20*$^{+/+}$ mice (Figure 6e), whereas *Lck-Cre/IFT20*$^{f/f}$ mice were strongly protected against CIA histopathology (Figure 6b).

© 2014 Sichuan University

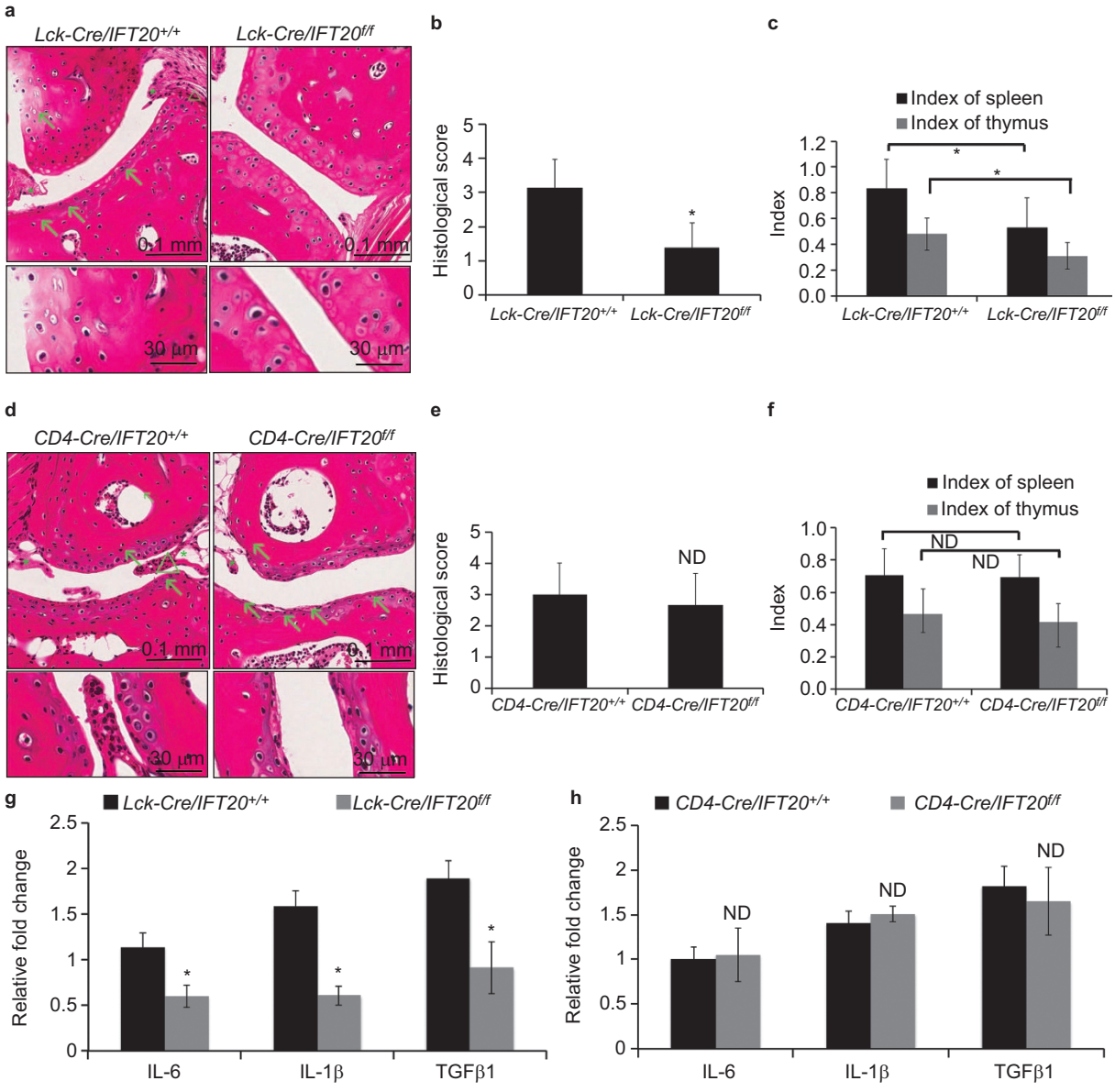

Figure 6. Deletion of IFT20 protected against histopathological progression of arthritis in *Lck-Cre/IFT20$^{f/f}$* mice, but not in *CD4-Cre/IFT20$^{f/f}$* mice. (**a**) Representative H&E-stained section of interphalangeal joints from *Lck-Cre/IFT20$^{+/+}$* and *Lck-Cre/IFT20$^{f/f}$* mice. Synovial hyperplasia and pannus formation were inhibited and destruction of articular cartilage was alleviated in *Lck-Cre/IFT20$^{f/f}$* mice. Arrow indicates cartilage destruction; Δ indicates infiltration of inflammatory cells; * indicates fibrovascular synovial and periarticular proliferation. (**b**) The histopathological change was scored and data is expressed as mean ± S.D. for each group of 6 samples (n=6, P<0.01). (**c**) Indices of thymus and spleen in CIA in *Lck-Cre/IFT20$^{+/+}$* and *Lck-Cre/IFT20$^{f/f}$* mice (n=8). (**d**) Representative H&E-stained section of interphalangeal joints from *CD4-Cre/IFT20$^{+/+}$* and *CD4-Cre/IFT20$^{f/f}$* mice. (**e**) Histological scores of synovial inflammation and cartilage erosion was shown as mean±s.d. (n=6). (**f**) Indices of thymus and spleen in collagen-induced arthritis in *CD4-Cre/IFT20$^{+/+}$* and *CD4-Cre/IFT20$^{f/f}$* mice (n=8). (**g**) Comparison of IL-1, IL-6 and TGF-β1 mRNA levels in the hind paws of *Lck-Cre/IFT20$^{+/+}$* and *Lck-Cre/IFT20$^{f/f}$* mice (n=4, P<0.01). (**h**) Comparison of IL-1, IL-6 and TGF-β1 mRNA levels in the hind paws of *CD4-Cre/IFT20$^{+/+}$* and *CD4-Cre/IFT20$^{f/f}$* mice (n=4). ND indicated no significantly difference. H&E, hematoxylin and eosin.

The thymus and spleen were weighed to calculate the respective indices at the end of the experiments. Results showed that thymus and spleen indices were higher in *Lck-Cre/IFT20$^{+/+}$* mice compared to *Lck-Cre/IFT20$^{f/f}$* mice (Figure 6c). However, these indices were not greatly different in *CD4-Cre/IFT20$^{f/f}$* mice compared to *CD4-Cre/IFT20$^{+/+}$* mice (Figure 6f).

To further confirm the degree of inflammation and cartilage degradation of the joint in the CIA mice, we performed the qPCR to detect expression of IL-1β, IL-6 and TGF-β1 in the paw. IL-1β is a crucial cytokine that mediates both arthritis and cartilage destruction.[41] IL-6, which participates in the pathogenesis of RA, is the most powerful pro-inflammatory cytokine.[42] TGF-β1 is highly expressed in the

© 2014 Sichuan University

later stages of CIA.[43–44] Total RNA from the paw was harvested as described in the section on 'Materials and methods'. qPCR results indicated that expression of IL-1β, IL-6 and TGF-β1 were all significantly lower in the paw of *Lck-Cre/IFT20$^{f/f}$* mice (Figure 6g). As expected, the expression of IL-1β, IL-6 and TGF-β1 was not significantly different in *CD4-Cre/IFT20$^{f/f}$* compared to *CD4-Cre/IFT20$^{+/+}$* mice (Figure 6h).

DISCUSSION

IFT proteins are known to form IFT complexes A and B. These proteins interact with other proteins to build cilia and maintain cilia function.[45] Mutations of IFT or defects in cilia that have been implicated in human disease are called ciliopathies.[46–47] These effects of these mutations demonstrate the critical role of primary cilia and IFT proteins in organ development and function.

Hematopoietic lineage cells are an exception, however, because they lack cilia.[45,48] The reason is not yet known. However, Finetti *et al*.[14] recently discovered that IFT20 was expressed in both lymphoid and myeloid lineage cells, suggesting a role of IFT proteins beyond cilia development and function. In most eukaryotic cells, IFT20 is localized in cilia, the centrioles, and the Golgi. IFT20 selects and marks vesicles, which contain ciliary proteins, and later assembles these with IFT complexes and transports them within the cilium.[49] In T lymphocytes, IFT20 is associated with the centriole, Golgi and post-Golgi membrane compartments and required for TCR/CD3 trafficking and immune synapse formation in T lymphocytes in antigen-specific conjugates.[14] Other IFT proteins, such as IFT88 and IFT57, along with IFT-dependent motor kinesin-2, are also expressed in lymphoid and myeloid cells.[14] These findings suggest that all or some of the IFT proteins could exist and function in T cells, supporting the theory that the immune synapse may be a type of 'frustrated cilium' and share similar molecular mechanisms.[48] Immune synapse formation facilitates detailed antigen recognition and effective T-cell responses and, thus, is important for T-cell activation.[50–51] Knockdown of *IFT20* inhibits TCR recycling and disrupts synapse formation *in vitro*.[14] However, the role of IFT20 in regulating T-cell development and activation *in vivo* is largely unknown. Our study, for the first time, analyzed the role of IFT20 in T cells in a mouse CIA model.

In our study, we crossed *IFT20$^{f/f}$* mice with Lck-Cre and CD4-Cre mice to delete *IFT20* in the T-cell lineage at early and later stages. Both Lck-Cre and CD4-Cre transgenic lines have been extensively used in the studies of lymphoid progenitors at different developmental stages,[38–39] which have shown that these lines can delete genes at specific early and later stages of T-cell development. The major stages of T-cell maturation in the thymus are DN ($CD4^-CD8^-$), DP ($CD4^+CD8^+$) and SP ($CD4^+$ or $CD8^+$) (Figure 1a). Lck-Cre mediated deletion occurs in the DN stage and CD4-Cre targeted deletion begins later in the DP stage. We confirmed that the IFT20 gene was efficiently deleted in both *Lck-Cre/IFT20$^{f/f}$* and *CD4-Cre/IFT20$^{f/f}$* mice. Both *Lck-Cre/IFT20$^{f/f}$* and *CD4-Cre/IFT20$^{f/f}$* mice were normal and healthy without any significant defects in thymus or spleen size (Figure 2). However, we found deletion of *IFT20* with Lck-Cre arrested T cells further along in development than the DP stage (Figure 3a and 3b). When the cells go through the DN2 to DN4 stages, they express the pre-TCR. Successful pre-TCR expression and translocation to the cell surface is required for DN4 to DP transition. This is called beta-selection.[52–53] Since IFT20 involvement in transportation is important for the TCR expression, deletion of *IFT20* may cause partial impairment of passing beta-selection. Unexpectedly, CD4-Cre-mediated *IFT20* deletion did not apparently affect DP T-cell differentiation to SP T cells, indicating IFT20 likely does not function or play a minor role in T-cell maturation.

Studies of our CIA mouse models have shown that T-cell activation is important in the initiation and pathogenesis of inflammatory arthritis.[54] To investigate whether loss of IFT20 in T-cell lineage affects T-cell development and activation, we employed a mouse CIA model in wild-type and *IFT20* mutant mice. Chicken type II collagen can activate collagen-specific T cells with the help of antigen-presenting cells, leading the activated T cells to cross-react with and damage the body's own type II collagen through activation of B cells and other immune cells. We found that *Lck-Cre/IFT20$^{f/f}$* mice were resistant to chicken type II collagen-induced arthritis. *Lck-Cre/IFT20$^{f/f}$* mice had significantly lower average and maximum clinical arthritis scores, inflammation scores and paw thicknesses compared to *Lck-Cre/IFT20$^{+/+}$* mice. This data confirmed that *IFT20* deficiency from an early stage of thymocyte differentiation blocked functional T-cell formation and eventually inhibited T-cell response to the collagen challenge. Surprisingly, *CD4-Cre/IFT20$^{f/f}$* mice had no significant difference from *CD4-Cre/IFT20$^{+/+}$* mice in this respect. In addition to the CIA model, we have also challenged *Lck-Cre/IFT20$^{f/f}$* and *CD4-Cre/IFT20$^{f/f}$* mice with *Borrelia burgdorferi* to induce Lyme disease and associated destructive arthritis.[55] The role of T cells in development and exacerbation of Lyme disease has been defined.[56] Consistent with our CIA results, *Lck-Cre/IFT20$^{f/f}$* mice have less inflammation in paw joints while *CD4-Cre/IFT20$^{f/f}$* did not display any significant difference from *CD4-Cre/IFT20$^{+/+}$* in response to *Borrelia burgdorferi* challenge (unpublished data), suggesting IFT20 likely plays a more important role in the early stage of T-cell differentiation.[57]

Cytokines are involved in primary cartilage damage and synovial activation of osteoarthritis. Our data has shown that T cells from CIA models of wild-type and *IFT20* mutant mice (Lck-Cre or CD4-Cre) can be subjected to

© 2014 Sichuan University

antigen-specific (type II collagen) proliferation and cytokine production.[58] IL-1 is a potent pro-inflammatory cytokine, which is capable of inducing chondrocytes and synovial cells to synthesize the matrix metalloproteinases, which are responsible for the degradation of cartilage. TGF-β is well-characterized as a potent chondrocyte growth factor. TGF-β not only stimulates de novo matrix synthesis, but also counteracts cartilage degradation by down-regulating IL-1 receptor expression and by increasing both IL-1 receptor antagonist release and the expression of tissue inhibitors of matrix metalloproteinases. IL-6 is the most powerful pro-inflammatory cytokine which participates in the pathogenesis of RA.[42] By analyzing these cytokines, we found that the expression of IL-1β, IL-6 and TGF-β1 was significantly decreased in the paw of *Lck-Cre/IFT20$^{f/f}$* mice (Figure 6g). These finding demonstrate that IFT20 plays crucial role in the early stage of T-cell differentiation and function. In the late stage of T-cell differentiation, IFT20 did not markedly affect T-cell maturation and the response of T cells to type II collagen antigen. Consistent with these finding, the expression of IL-1β, IL-6 and TGF-β were not significantly different in *CD4-Cre/IFT20$^{f/f}$* compared to *CD4-Cre/IFT20$^{+/+}$* (Figure 6h). Our *in vivo* results identify that IFT20 is an important regulator in T-cell early stage differentiation and function and provide the first evidence to implicate IFT20 might be unimportant for late stage of CD4 T-cell maturation and function.

Competing interests

The authors declare no conflict of interest.

Acknowledgements

The authors thank Miss Stacy Scheuneman for editing the manuscript, and thank Dr Raymond J. Kelleher, the director of the Flow Cytometry Facility at the School of Medicine and Biomedical Sciences, University at Buffalo, for assistance with the flow cytometry. Research reported in this publication was supported by the National Institute of Arthritis and Musculoskeletal and Skin Diseases, part of the National Institutes of Health, under Award Numbers AR055678, DE023105 and AR061052 to SY. The content is solely the responsibility of the authors and does not necessarily represent the official views of the National Institutes of Health.

References

1 KozMinski KG, Johnson KA, Forscher P, Rosenbaum JL. A motility in the eukaryotic flagellum unrelated to flagellar beating. *Proc Natl Acad Sci USA* 1993; **90**: 5519–5523.
2 Rosenbaum JL, Witman GB. Intraflagellar transport. *Nat Rev Mol Cell Biol* 2002; **3**: 813–825.
3 Taschner M, Bhogaraju S, Lorentzen E. Architecture and function of IFT complex proteins in ciliogenesis. *Differentiation* 2012; **83**: S12–S22.
4 Cole DG, Diener DR, Himelblau AL, Beech PL, Fuster JC, Rosenbaum JL. *Chlamydomonas kinesin*-II-dependent intraflagellar transport (IFT): IFT particles contain proteins required for ciliary assembly in *Caenorhabditis elegans* sensory neurons. *J Cell Biol* 1998; **141**: 993–1008.
5 Cole DG, Snell WJ. SnapShot: intraflagellar transport. *Cell* 2009; **137**: 784–784.e1.
6 Piperno G, Siuda E, Henderson S, Segil M, Vaananen H, Sassaroli M. Distinct mutants of retrograde intraflagellar transport (IFT) share similar morphological and molecular defects. *J Cell Biol* 1998; **143**: 1591–1601.
7 Ishikawa H, Marshall WF. Ciliogenesis: building the cell's antenna. *Nat Rev Mol Cell Biol* 2011; **12**: 222–234.
8 Pedersen LB, Rosenbaum JL. Intraflagellar transport (IFT) role in ciliary assembly, resorption and signalling. *Curr Top Dev Biol* 2008; **85**: 23–61.
9 Orozco JT, Wedaman KP, Signor D, Brown H, Rose L, Scholey JM. Movement of motor and cargo along cilia. *Nature* 1999; **398**: 674.
10 Follit JA, San Agustin JT, Xu F *et al*. The Golgin GMAP210/TRIP11 anchors IFT20 to the Golgi complex. *PLoS Genet* 2008; **4**: e1000315.
11 Follit JA, Tuft RA, Fogarty KE, Pazour GJ. The intraflagellar transport protein IFT20 is associated with the Golgi complex and is required for cilia assembly. *Mol Biol Cell* 2006; **17**: 3781–3792.
12 Baker SA, Freeman K, Luby-Phelps K, Pazour GJ, Besharse JC. IFT20 links kinesin II with a mammalian intraflagellar transport complex that is conserved in motile flagella and sensory cilia. *J Biol Chem* 2003; **278**: 34211–34218.
13 Cesari F. Membrane trafficking: IFT proteins play a new game. *Nat Rev Mol Cell Biol* 2009; **10**: 812.
14 Finetti F, Paccani SR, Riparbelli MG *et al*. Intraflagellar transport is required for polarized recycling of the TCR/CD3 complex to the immune synapse. *Nat Cell Biol* 2009; **11**: 1332–1339.
15 Jonassen JA, San Agustin J, Follit JA, Pazour GJ. Deletion of IFT20 in the mouse kidney causes misorientation of the mitotic spindle and cystic kidney disease. *J Cell Biol* 2008; **183**: 377–384.
16 Keady BT, Le YZ, Pazour GJ. IFT20 is required for opsin trafficking and photoreceptor outer segment development. *Mol Biol Cell* 2011; **22**: 921–930.
17 McInnes IB, Schett G. The pathogenesis of rheumatoid arthritis. *N Engl J Med* 2011; **365**: 2205–2219.
18 Brand DD, Latham KA, Rosloniec EF. Collagen-induced arthritis. *Nat Protoc* 2007; **2**: 1269–1275.
19 Brand DD. Rodent models of rheumatoid arthritis. *Comp Med* 2005; **55**: 114–122.
20 Asquith DL, Miller AM, McInnes IB, Liew FY. Animal models of rheumatoid arthritis. *Eur J Immunol* 2009; **39**: 2040–2044.
21 Inglis JJ, Criado G, Medghalchi M *et al*. Collagen-induced arthritis in C57BL/6 mice is associated with a robust and sustained T-cell response to type II collagen. *Arthritis Res Ther* 2007; **9**: R113.
22 Seetharaman R, Mora AL, Nabozny G, Boothby M, Chen J. Essential role of T cell NF-κB activation in collagen-induced arthritis. *J Immunol* 1999; **163**: 1577–1583.
23 Nakahama T, Kimura A, Nguyen NT *et al*. Aryl hydrocarbon receptor deficiency in T cells suppresses the development of collagen-induced arthritis. *Proc Natl Acad Sci USA* 2011; **108**: 14222–14227.
24 Chung SH, Seki K, Choi BI *et al*. CXC chemokine receptor 4 expressed in T cells plays an important role in the development of collagen-induced arthritis. *Arthritis Res Ther* 2010; **12**: R188.
25 Jonassen JA, San Agustin J, Follit JA, Pazour GJ. Deletion of IFT20 in the mouse kidney causes misorientation of the mitotic spindle and cystic kidney disease. *J Cell Biol* 2008; **183**: 377–384.
26 Yang S, Li YP, Liu T *et al*. Mx1-Cre mediated Rgs12 conditional knockout mice exhibit increased bone mass phenotype. *Genesis* 2013; **51**: 201–209.
27 Campbell IK, Hamilton JA, Wicks IP. Collagen-induced arthritis in C57BL/6 (H-2b) mice: new insights into an important disease model of rheumatoid arthritis. *Eur J Immunol* 2000; **30**: 1568–1575.
28 Liu Y, Zhang L, Wu Y *et al*. Therapeutic effects of TACI-Ig on collagen-induced arthritis by regulating T and B lymphocytes function in DBA/1 mice. *Eur J Pharmacol* 2011; **654**: 304–314.

© 2014 Sichuan University

29 Taneja V, Taneja N, Paisansinsup T *et al*. CD4 and CD8 T cells in susceptibility/protection to collagen-induced arthritis in HLA-DQ8-transgenic mice: implications for rheumatoid arthritis. *J Immunol* 2002; **168**: 5867–5875.
30 Kwon OG, Ku SK, An HD, Lee YJ. The Effects of Platycodin D, a Saponin Purified from Platycodi Radix, on Collagen-Induced DBA/1J Mouse Rheumatoid Arthritis. *Evid Based Complement Alternat Med* 2014; **2014**: 954508.
31 Liu Y, Zhang L, Wu Y *et al*. Therapeutic effects of TACI-Ig on collagen-induced arthritis by regulating T and B lymphocytes function in DBA/1 mice. *Eur J Pharmacol* 2011; **654**: 304–314.
32 Tong T, Zhao W, Wu YQ *et al*. Chicken type II collagen induced immune balance of main subtype of helper T cells in mesenteric lymph node lymphocytes in rats with collagen-induced arthritis. *Inflamm Res* 2010; **59**: 369–377.
33 Zhang LL, Wei W, Yan SX, Hu XY, Sun WY. Therapeutic effects of glucosides of Cheanomeles speciosa on collagen-induced arthritis in mice. *Acta Pharmacol Sin* 2004; **25**: 1495–1501.
34 Stordeur P, Poulin LF, Craciun L *et al*. Cytokine mRNA quantification by real-time PCR. *J Immunol Methods* 2002; **259**: 55–64.
35 Hochrainer K, Racchumi G, Anrather J. Site-specific phosphorylation of the p65 protein subunit mediates selective gene expression by differential NF-κB and RNA polymerase II promoter recruitment. *J Biol Chem* 2013; **288**: 285–293.
36 Chu CY, Peng FC, Chiu YF *et al*. Nanohybrids of silver particles immobilized on silicate platelet for infected wound healing. *PLoS One* 2012; **7**: e38360.
37 Kisielow P, von Boehmer H. Development and selection of T cells: facts and puzzles. *Adv Immunol* 1995; **58**: 87–209.
38 Lee PP, Fitzpatrick DR, Beard C *et al*. A critical role for Dnmt1 and DNA methylation in T cell development, function, and survival. *Immunity* 2001; **15**: 763–774.
39 Shi J, Petrie HT. Activation kinetics and off-target effects of thymus-initiated cre transgenes. *PLoS One* 2012; **7**: e46590.
40 Guedez YB, Whittington KB, Clayton JL *et al*. Genetic ablation of interferon-gamma up-regulates interleukin-1beta expression and enables the elicitation of collagen-induced arthritis in a nonsusceptible mouse strain. *Arthritis Rheum* 2001; **44**: 2413–2424.
41 Lubberts E, van den Berg WB. Cytokines in the pathogenesis of rheumatoid arthritis and collagen-induced arthritis. *Adv Exp Med Biol* 2003; **520**: 194–202.
42 Yusof MYM, Emery P. Targeting interleukin-6 in rheumatoid arthritis. *Drugs* 2013; **73**: 341–356.
43 Marinova-Mutafchieva L, Gabay C, Funa K, Williams R. Remission of collagen-induced arthritis is associated with high levels of transforming growth factor-β expression in the joint. *Clin Exp Immunol* 2006; **146**: 287–293.
44 Thornton S, Duwel LE, Boivin GP, Ma Y, Hirsch R. Association of the course of collagen-induced arthritis with distinct patterns of cytokine and chemokine messenger RNA expression. *Arthritis Rheum* 1999; **42**: 1109–1118.
45 Pazour GJ, Witman GB. The vertebrate primary cilium is a sensory organelle. *Curr Opin Cell Biol* 2003; **15**: 105–110.
46 Eggenschwiler JT, Anderson KV. Cilia and developmental signaling. *Annu Rev Cell Dev Biol* 2007; **23**: 345–373.
47 Goetz SC, Anderson KV. The primary cilium: a signalling centre during vertebrate development. *Nat Rev Genet* 2010; **11**: 331–344.
48 Finetti F, Paccani SR, Rosenbaum J, Baldari CT. Intraflagellar transport: a new player at the immune synapse. *Trends Immunol* 2011; **32**: 139–145.
49 Nachury MV, Seeley ES, Jin H. Trafficking to the ciliary membrane: how to get across the periciliary diffusion barrier? *Annu Rev Cell Dev Biol* 2010; **26**: 59–87.
50 Grakoui A, Bromley SK, Sumen C *et al*. The immunological synapse: a molecular machine controlling T cell activation. *Science* 1999; **285**: 221–227.
51 Dustin ML, Chakraborty AK, Shaw AS. Understanding the structure and function of the immunological synapse. *Cold Spring Harb Perspect Biol*. 2010 Oct; **2**(10): a002311.
52 Germain RN. T-cell development and the CD4–CD8 lineage decision. *Nat Rev Immunol* 2002; **2**: 309–322.
53 Hernandez JB, Newton RH, Walsh CM. Life and death in the thymus—cell death signaling during T cell development. *Curr Opin Cell Biol* 2010; **22**: 865–871.
54 Tran CN, Lundy SK, Fox DA. Synovial biology and T cells in rheumatoid arthritis. *Pathophysiology* 2005; **12**: 183–189.
55 Sze CW, Zhang K, Kariu T, Pal U, Li C. Borrelia burgdorferi needs chemotaxis to establish infection in mammals and to accomplish its enzootic cycle. *Infect Immun* 2012; **80**: 2485–2492.
56 McKisic MD, Redmond WL, Barthold SW. Cutting edge: T cell-mediated pathology in murine *Lyme borreliosis*. *J Immunol* 2000; **164**: 6096–6099.
57 Onoyama I, Tsunematsu R, Matsumoto A *et al*. Conditional inactivation of Fbxw7 impairs cell-cycle exit during T cell differentiation and results in lymphomatogenesis. *J Exp Med* 2007; **204**: 2875–2888.
58 Ellebedy AH, Lupfer C, Ghoneim HE, DeBeauchamp J, Kanneganti TD, Webby RJ. Inflammasome-independent role of the apoptosis-associated speck-like protein containing CARD (ASC) in the adjuvant effect of MF59. *Proc Natl Acad Sci U S A* 2011; **108**: 2927–2932.

This work is licensed under a Creative Commons Attribution-NonCommercial-ShareAlike 3.0 Unported License. The images or other third party material in this article are included in the article's Creative Commons license, unless indicated otherwise in the credit line; if the material is not included under the Creative Commons license, users will need to obtain permission from the license holder to reproduce the material. To view a copy of this license, visit http://creativecommons.org/licenses/by-nc-sa/3.0/